Journal of Thermal Analysis and Calorimetry, Vol. 96 (2009) 1, 15–20

LIGAND EFFECTS ON THE SIZE AND PURITY OF Pd NANOPARTICLES

M. Iqbal[1], *J. McLachlan*[1], *W. Jia*[1], *N. Braidy*[2], *G. Botton*[2] *and S. H. Eichhorn*[1*]

[1]Department of Chemistry and Biochemistry, University of Windsor, Windsor, Ontario, Canada
[2]McMaster University, Engineering, Materials Science and Engineering, Brockhouse Institute of Materials Research, Hamilton Ontario, L8S 4M1, Canada

Palladium nanoparticles (Pd-NPs) were prepared by a single-phase reduction of palladium acetate in the presence of different organic thiol ligands. Sizes, size distributions and crystallinity of the Pd-NPs were determined by high resolution transmission electron microscopy (HR-TEM) and powder X-ray diffraction (XRD) while thermogravimetric analysis coupled with mass spectroscopy (TGA-MS) was employed to measure their organic ligand to palladium ratios and to quantify contaminants. No systematic effect of the different ligands on the size and purity of the Pd-NPs was observed but 1st-generation Frechet dendron thiols had an about 4 times larger foot-print at the surface of the NPs than the other thiol ligands.

Keywords: *mass spectrometry, nanoparticles, palladium, solution synthesis, TG, TG-MS, X-ray diffraction*

Introduction

Surface protected soluble noble metal nanoparticles (NPs) have become ubiquitous building blocks for nano-sized materials and are commercially available as markers in biochemistry and molecular biology [1–3]. Proposed applications include their use as catalysts [4–6], semiconductors [7] and sensors [8]. Many of their properties are adjustable by attaching different types of organic molecules to the surface of the metal NP. Thiols are most often used but several other functional groups have been shown to also adsorb sufficiently well onto the metal surfaces [2].

Fast and reliable characterization of metal nanoparticles remains a challenge especially as most synthetic approaches generate compound mixtures rather than nanoparticles of only one composition. Information on size and size distributions of the metal cores is usually based on TEM measurements [9], which necessarily consider only a limited number of particles. Powder XRD probes the size distribution of bulk quantities but the extraction of accurate values for core sizes based on line broadening is complicated by other contributing factors such as number of defects and distortions from the perfect crystal lattice [10–12].

Energy dispersive X-ray (EDX) [13] analyses and X-ray photoelectron spectroscopy (XPS) [14–16] provide information on the composition of the metal core as well as on the molecules and ions that are adsorbed to the surface of the metal nanoparticles. Quantitative analysis of elemental ratios is possible but depends on the sample preparation, the penetration depth of the measurement and the type of elements under investigation. Alternatively, the compositions of the metal cores and their protective layers may be determined by conventional elemental analysis but the metal content may complicate measurements and a relatively large quantity of compound is required for measuring a range of different elements [17, 18].

Thermogravimetry (TG) has been routinely employed for the quantification of organic *vs.* metal content based on the assumption that all the attached molecules and ions are thermally removed and that no metal atoms evaporate [17, 19, 20]. TG alone does not provide any information on the type of compounds that are thermally removed and additional measurements such as thermal desorption mass spectrometry have been employed for this purpose [17]. Our group recently reported on the characterization of gold and palladium nanoparticles by combining TG and mass spectrometry (TG-MS) [18]. The report also outlined the importance of high temperature TG measurements (>700°C) to ensure a quantitative removal of all compounds attached to the surfaces of the nanoparticles. Some nanoparticles showed up to 3 distinct mass loss events that could be determined as subsequent losses of thiol ligands, inorganic salts and oxidised sulphur species by MS analysis of the evolved gases.

Presented here is the synthesis and characterization of Pd-NPs containing thiol ligands with straight aliphatic chains and branched chains as well as a 1st-generation Frechet-type dendron (Scheme 1). Increase of the bulk of the organic groups is expected to reduce the core size of the Pd-NPs, increase the con-

* Author for correspondence: eichhorn@uwindsor.ca

1388–6150/$20.00

Akadémiai Kiadó, Budapest, Hungary
Springer, Dordrecht, The Netherlands

tent of contaminants, lower the stability of the NPs, and increase the foot-prints of the ligands on the surface of the NPs.

Experimental

Materials and methods

1-Dodecanethiol (98+%), 2-methyl-1-propanethiol (92%), 2-methyl-2-propanethiol (99%), phenylethanethiol (98%), lithium triethylborohydride (Super-Hydride®, 1.0 M in THF), palladium(II) acetate (99.9%) were purchased from Aldrich and used as obtained. The 1st-generation Frechet-type dendron thiol was prepared following a previously reported procedure [21, 22]. All solvents were used as obtained except for THF, which was distilled from sodium or obtained from a Grubbs' type solvent purification system by Innovative Technology and filtered through a 0.2 μm PTFE filter prior to use.

Synthesis of palladium nanoparticles

All nanoparticles were synthesized using the single phase method [23]. In a general procedure palladium(II) acetate (0.224 g, 1 mmol) was dissolved in 30 mL of dry THF and 3 mL of dried and degassed acetonitrile at room temperature. The reaction mixture was purged with argon gas and 2.5 eq. of the thiol was added at 0°C. A 1M solution of Super-Hydride® in THF (10 mL) was added after 30 min via a syringe pump at a rate of 45 mL h^{-1}. The reaction was quenched after 2 h by the addition of 100 mL of ethanol (95%) under argon.

The precipitated Pd-NPs were removed by centrifugation in PTFE tubes, re-suspended in ethanol and again centrifuged off. This washing step was performed two more times before the Pd-NPs were dissolved in 20 mL of THF and precipitated out by the addition of 100 mL of a 1:1 solution of methanol/water. The final precipitate was collected on a 0.45 μm PTFE filter, washed with 20 mL of a 1:1 solution of acetone/water as well as 20 mL of methanol and finally dried in vacuum (1 mbar) for 24 h. The absence of free thiol groups was verified by IR spectroscopy measurements.

In situ ligand exchange of Pd-NPs prepared in the presence of *iso*-butyl and *tert*-butyl thiols was achieved by the addition of 10 eq. of 1-dodecanethiol to half of the reduced reaction mixture. The mixture was allowed to stir for 24 h before it was quenched with ethanol and purified as described above to give samples 3ex and 4ex.

Characterization of palladium nanoparticles

Transmission electron microscopy (HR-TEM) was performed on a JEOL 2010F FEG TEM/STEM operated at an accelerating voltage of 200 kV at McMaster University. Dilute solutions of NPs in THF were filtered through a 0.02 μm filter, dropped onto a carbon-coated copper grid (200 mesh, SPI Supplies) and the solvent was allowed to evaporate. Reported size distributions are based on the measurements of at least 100 particles per sample and particle sizes below 2 nm were determined by annular dark field STEM. TEM samples of 3 and 4 were prepared from the reaction solution because their isolated powders did not fully re-dissolve. Thermal gravimetric analysis with mass spectrometric detection of evolved gases was conducted on a Mettler Toledo TG SDTA 851^e that was attached to a Pfeiffer Vacuum Thermostar™ mass spectrometer (1–300 amu) via a thin glass capillary. Helium (99.99%) was used to purge the system with a flow rate of 60 mL min^{-1}. Samples were held at 25 or 30°C for 30 min before they were heated to 1100°C at a rate of 2°C min^{-1} or 1000°C at a rate of 5°C min^{-1}. A mass range between 16 and 200 *m*/*z* was constantly scanned. All powder XRD's were run on a Bruker D8 Discover diffractometer with a GADDS 2D-detector operating at 40 kV and 40 mA. CuK_{α_1} radiation (λ=1.54187 Å) with an initial beam of 0.5 mm in diameter was used. All samples where sealed in Charles Supper Company 1.0 mm glass capillaries and run for 2 h each at 2θ values of 18, 50 and 80°. UV-VIS spectra of solutions in THF (spectroscopic grade) were recorded on a Varian Cary 50 and corrected for solvent absorption.

Results and discussion

Synthesis of palladium nanoparticles

Pd-NPs 1-5 (Scheme 1) were prepared in a single phase and surfactant free reaction mixture following a previously reported procedure [23]. They were isolated as dark gray to black powders while their solutions in THF were brown in colour. Dried powders of Pd-NPs 1, 2, 5 could be quantitatively re-dissolved in THF but 3 and 4 became insoluble after being fully dried. Clearly, the *tert*-butyl and *iso*-butyl thiols only provide limited protection against aggregation and coagulation of the NP cores. For this reason parts of the reaction mixtures of 3 and 4 were in situ treated with excess dodecane thiol to quantitatively exchange the *iso*-butyl and *tert*-butyl thiol ligands before they were isolated as powders to give the stable NPs 3ex and 4ex, respectively.

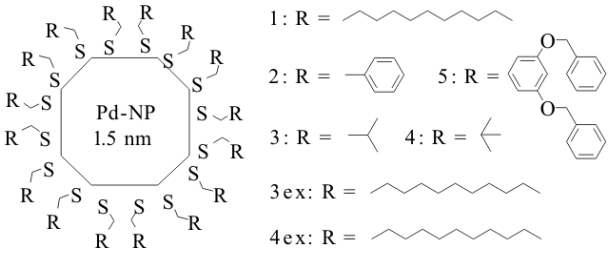

Scheme 1 Organic thiol ligands employed in the synthesis of Pd-NPs

UV-Vis, TEM and XRD analysis of the Pd-NPs

A weak surface plasmon resonance peak is observed for 2 at 380 nm while 1 and 3ex show weak and broad peaks near 320 and 410 nm (Fig. 1). All other NPs do not display observable surface plasmon resonance peaks between 250 and 1000 nm but all NPs showed the featureless exponential increase in absorption that is typical for metal nanoparticles in the size range between 1–10 nm. Values between 225 and 302 nm have been reported in the literature for Pd NPs of sizes of 3–4 nm [20, 23] but absorptions near 350 and 400 nm have also been reported and are similar to absorptions found for S containing Pd(II) complexes [24]. However, the surface plasmon resonance peak appears to be less predictable in Pd NPs than it is in Au-NPs and consequently difficult to use for analytical purposes.

HR-TEM measurements confirmed the presence of Pd-NPs of average sizes between 1.5–2.7 nm (Table 1). NPs of sizes well below 2 nm required dark field imaging (STEM) as shown in Fig. 2 because their contrast is much lower than that of similarly sized Au-NPs. No significant effect of the different ligands on the sizes of the Pd-NPs is observed. Pd-NPs 3 and 3ex have slightly larger sizes, which is attributed to the low stability of 3 in solution rather than differences in growth. The lower stability of *iso*-butyl thiol and, to a lesser degree, *tert*-butyl thiol protected NPs 3 and 4 is also reflected in their larger size distributions. TEM of 3 and 4 (reaction solution) as well as 3ex and 4ex confirm that the in-situ exchange of *iso*- and *tert*-butyl thiol ligands by dodecane thiol occurs without significant change of the size and size distribution of the palladium cores.

Powder XRD of the Pd-NPs gave peaks in the small angle and in the wide angle regions (Fig. 3). Reflections below 2θ=5° are attributed to the ordered packing of the NPs and their packing distance depends on both the size of the palladium cores and the thickness of the attached organic layers. Pd-NP 1 has the smallest angle reflection at 3.0 nm followed by 2, 5, 3 and 4 with values of 2.1, 2.1, 1.9 and 1.7 nm, respectively. A reflection at 2.7 nm is found for Pd-NP 3ex and 4ex (not shown).

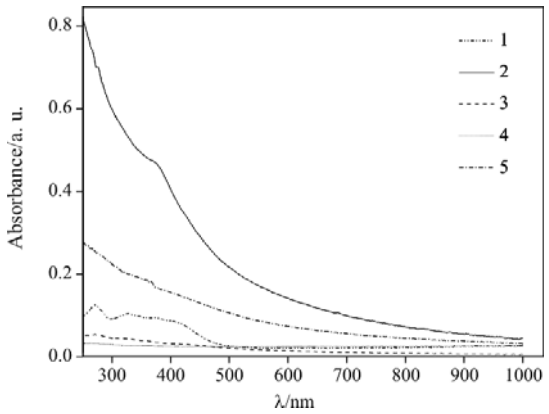

Fig. 1 UV/Vis spectra of reaction solutions of 1, 2, 3, 4 and 5 in THF

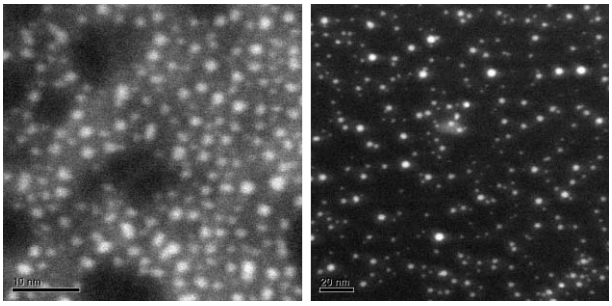

Fig. 2 Annular dark field STEM images of Pd-NPs 5 (left, scale bar is 10 nm) and 3ex (right, scale bar is 20 nm)

Table 1 Average sizes and their standard deviations of the Pd cores of all Pd-NPs based on TEM analysis

Pd-NP	Average diameter/ nm, ±0.1	Standard deviation	Estimated number of Pd atoms and diameters/(nm[a])
1	2.0	0.3	147 (1.9)
2	1.5	0.4	55 (1.4)
3	2.2	0.8	228[b]
4	1.9	0.5	147 (1.9)
5	1.6	0.2	55 (1.4)
3ex	2.5	1.0	309 (2.5)
4ex	1.7	0.3	101[b]

[a]This estimation is based on a FCC structure of the palladium core and the presence of full shells (magic numbers) [25]. Two shells contain 55 palladium atoms, 3 shells 147 and 4 shells 309 atoms. [b]These sizes are in-between two shells and the number was calculated by dividing the sum of atoms for the next smaller and larger shells by two

The lattice of the packing could not be determined because only one intense reflection is observed but an FCC packing may be assumed and the observed peaks would then represent (111) reflections. Based on this assumption distances between Pd NPs in samples 1, 2, 5, 3 and 4 are calculated to 4.2, 3.0, 3.0, 2.7, 2.4 nm, respectively. These are realistic val-

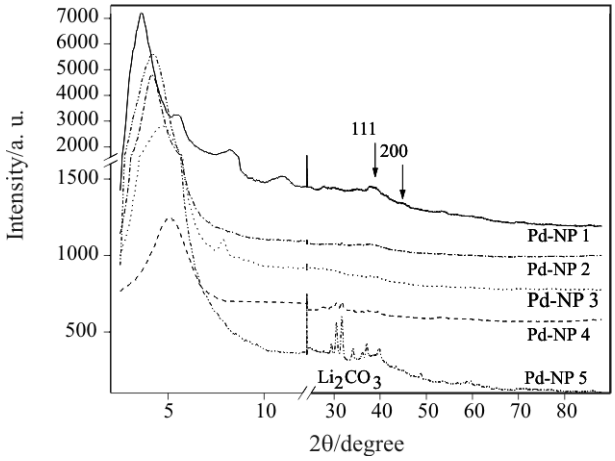

Fig. 3 Powder XRD patterns of Pd-NPs 1–5 at 25°C. Both axes contain breaks to allow enlargement of the important areas for clarity

ues considering the sizes of the cores as determined by HR-TEM and the length of the different thiol ligands. A larger inter-particle spacing may be expected for 5 in comparison to 2 based on the difference in length of the two ligands but another important factor that determines the spacing between NPs is the density of the organic coating. Dodecane thiol and ethylphenyl thiol of Pd-NPs 1 and 2 are expected to pack more densely than the dendron thiol and more dense packing results in less interpenetration of the organic layers when in contact.

Bulk palladium has an FCC lattice that gives rise to wide-angle reflections in XRD at 2θ values of 40° (100%), 46° (45%), 68° (25%), 82° (24%) and 86° (8%). [26] Weak and broad reflections at 38 and 44° are found in the diffraction patterns of Pd-NPs 1 and 3 while none of these peaks could be assigned with certainty for the other NPs. Both, the broadness and the lower intensity of the reflections indicate the presence of small NPs and an amorphous rather than a crystalline structure. Consequently, only the two most intense (111) and (002) reflections are seen for the largest NPs 1 and 3. The observed shift of their maxima to lower angles, when compared to bulk palladium, is in accordance with previously reported observations for Pd-NPs of this size range and reasoned with expanding inter-atomic distances [27].

The sharp peaks seen in the 2θ range between 30 to 40° of NPs 4 and 5 were identified as the diffraction pattern of crystalline Li_2CO_3 that is present in larger quantities. Li_2CO_3 is a typical contaminant in NPs prepared by this single phase method and can be detected in smaller quantities by TG-MS as discussed below.

TG-MS analysis of Pd-NPs

In a previous report we describe the importance of high temperature TG measurements and the advantage of MS analysis of the evolved gases in the characterization of gold and palladium nanoparticles [18]. As shown for Pd-NP 2 in Fig. 4 up to three distinct mass losses may be observed in these NPs: the loss of the organic groups between 100–250°C, the loss of CO_2 between 500–700°C generated by the thermal decomposition of inorganic carbonates such as Li_2CO_3, and at temperatures above 800°C the removal of other ionic contaminants as well as oxidized sulfur species derived from fragments of the organic ligands.

MS analysis of the evolved gases confirmed the above assignment of the three mass loss processes (Fig. 4). Shown are the concentration *vs.* temperature curves for signature ions at *m*/*z* values of 44 (CO_2) and 45 (CO_2H) indicating the decomposition of carbonates as well as at *m*/*z*=64 (SO_2) and *m*/*z*= 91(benzyl) indicating the decompositions of oxidized sulfur species and the ethyl benzene group, respectively. As shown in Fig. 4 the concentrations of each of these signature ion peaks significantly increased within the temperature range the mass losses occurred: 100–300°C for *m*/*z*=91, 500–600°C for *m*/*z*= 44 and 45, as well as 800–900°C for *m*/*z*=64.

Similar results were obtained for all other Pd-NPs and their TG curves are given in Fig. 5. The percent contributions of each of the three mass loss processes are presented in Table 2 that also includes estimated mass ratios of organic thiol ligands to Pd atoms for each NP. For these estimations the mass losses that occur above 500°C were subtracted from the total mass. This is not an accurate calculation because the loss between 500–700°C, mainly representing the decomposition of carbonate salts, only detects the loss of CO_2 while the formed metal oxides are not volatile at temperatures up to 1100°C and remain in the sample. The loss between

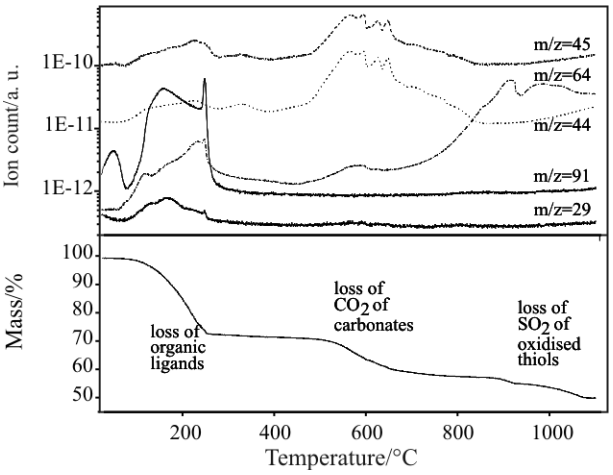

Fig. 4 TG curve of Pd-NP 2 showing three distinct mass loss events (bottom) and the simultaneously collected MS data (top, only selected ion concentrations are shown for clarity). The heating rate was 2°C min^{-1}

Table 2 Mass losses per temperature interval obtained by TG and the estimated organic thiol ligands to Pd core ratios

Pd-NP	Mass loss/%			Estimated organic to Pd ratio[a]/mass/mass	Relative molecular masses of thiol ligands
	25–500°C	500–700°C	700–1000°C		
1	49.1	6.6	9.1	1.4	2.2
2	41.6	1.1	5.6	0.8	1.5
3	31.4	0.5	5.2	0.5	1.0
4	36.9	9.0	8.9	0.8	1.0
5	35.4	1.5	4.8	0.6	3.7
3ex	62.7	0.5	4.0	1.9	2.2
4ex	58.3	0.8	2.2	1.5	2.2

[a]Mass losses above 500°C were subtracted from the total mass of the NPs

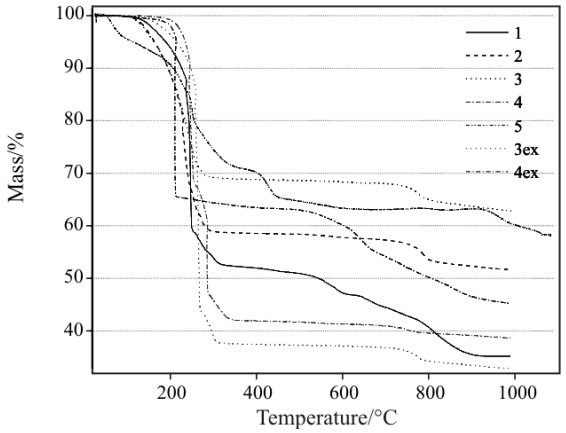

Fig. 5 TG curves of all seven Pd-NP samples showing up to three different temperature ranges at which mass loss occur. Measurements to 1000°C were conducted at 5°C min^{-1}, the measurement to 1100°C was conducted at 2°C min^{-1}

700–1100°C, on the other hand, likely contains fragments of the ligands and should be added to values for organic content. Since each of the two simplifications produce errors of less than 5% and their deviations from the correct value are of opposite directions, their subtraction should give correct values well within an error margin of ±5%.

Despite these simplifications and an estimated error margin of ±5% significant differences in thiol ligand to palladium ratios as well as contents of salts and oxidized sulfur compounds can be extracted from the TG-MS data. The highest ratios of thiol ligands to palladium are found in the dodecyl thiol containing NPs 1, 3ex, and 4ex. Ratios for Pd-NPs 2 to 5 are up to 70% lower but the masses of the thiol ligands of 2, 3 and 4 are also up to 55% lower so that a significantly less dense packing may only be concluded for 5. A comparison between NPs 5 and 4ex, both have comparable sizes and size distributions, reveals a fourfold increase in surface coverage per ligand in NP5 if both the organic to Pd ratio and the higher molecular mass of the dendron thiol are considered.

Compound 5 also shows the most complex loss of organic ligands of all the investigated Pd-NPs. At least three distinct steps between 80 and 400°C are resolved, which may be explained with distinctively different binding sites at the surfaces of the NPs. Differently bound thiol ligands should also be present in all other Pd-NPs but a denser packing of ligands and lower percent mass losses may blur the individual steps in mass loss. It has been proposed for thiol protected gold NPs that three different types of gold-thiol bonds may exist, the sulfur binding to 3 metal atoms as usually proposed for thiols on flat gold (111) surfaces, the sulfur binding to 2 metal atoms at edges of the surface, and the sulfur binding to only 1 metal atom at corner points of the surface of the NP [28]. However, very different types of binding between the gold surface of NPs and thiolate ligands may be obtained depending on the synthetic procedure and the type of thiolate ligand [29] and some differences have been observed for the binding of thiolates to Pd and gold surfaces [18].

No particular dependencies of the content of ionic contaminants and oxidized sulfur species on the types of thiol ligands are observed. NPs 1 and 4 have the highest contents but this is most likely caused by slight variations in the work-up, which crucially influence the formation and attachment of contaminants [18]. However, a comparison of NPs 3 and 4 with NPs 3ex and 4ex clearly shows that this ligand exchange is capable of removing contaminants. In fact, NPs 3ex and 4ex have higher organic to palladium ratios than analogous NP 1, which suggests that the higher content of contaminants in 1 reduces the content of thiol ligands by occupying surface sites.

Conclusions

Pd-NPs of sizes between 1.5 and 2.7 nm were prepared in a single phase reaction without surfactants in

the presence of different types of organic thiols. Size and size distributions varied but no systematic influence of the different organic groups on the sizes and purity of the Pd-NPs was observed. A much lower organic ligand to palladium ratio was measured for Pd-NPs 5 protected by 1st-generation Frechet dendron thiols. The foot-print of the dendron thiolates at the surface of the NPs was calculated to be about 4-times larger than for the other ligands. Pd-NPs 1, 2, 3, and 4 protected by dodecylthiols, phenylethanethiols, 2-methyl-1-propanethiol and 2-methyl-2-propanethiol, respectively, showed similar organic ligand to Pd ratios but NPs 3 and 4 are significantly less stable.

TG-MS at temperatures up to 1100°C has been demonstrated to be a versatile and convenient method for the characterization of mono-layer protected Pd-NPs. The method is capable of identifying and quantifying contents of contaminants, such as carbonate salts and fragments of oxidized thiol ligands, as well as differences in organic to palladium ratios. Information on the binding of ligands, however, is difficult to extract because of the complex thermal processes that may occur when the NPs are heated well beyond room temperature.

Acknowledgements

The authors thank Fred Pearson (McMaster) for help with TEM measurements as well as NSERC of Canada, CFI, OIT and OCE for funding.

References

1 M. Brust and C. J. Kiely, Colloids Surf., A, 202 (2002) 175.
2 M. C. Daniel and D. Astruc, Chem. Rev., 104 (2004) 293.
3 G. Schmid and B. Corain, Eur. J. Inorg. Chem., (2003) 3081.
4 J. D. Aiken and R. G. Finke, J. Mol. Catal. A: Chem., 145 (1999) 1.
5 C.-W. C. M. Akashi, Langmuir, 13 (1997) 6465.
6 C. Ornelas, J. R. Aranzaes, L. Salmon and D. Astruc, Chem.-Eur. J., 14 (2008) 50.
7 M. Brust, D. Bethell, C. J. Kiely and D. J. Schiffrin, Langmuir, 14 (1998) 5425.
8 X.-J. Huang and Y.-K. Choi, Sens. Actuators B: Chemical, 122 (2007) 659.
9 J. Y. Liu, J. Electron Microsc., 54 (2005) 251.
10 W. Lu, B. Wang, K. D. Wang, X. P. Wang and J. G. Hou, Langmuir, 19 (2003) 5887.
11 U. Schlotterbeck, C. Aymonier, R. Thomann, H. Hofmeister, M. Tromp, W. Richtering and S. Mecking, Adv. Funct. Mater., 14 (2004) 999.
12 G. Schmid, R. Pugin, T. Sawitowski, U. Simon and B. Marler, Chem. Commun., (1999) 1303.
13 V. Abdelsayed, G. Glaspell, M. Nguyen, J. M. Howe and M. S. El-Shall, Faraday Discuss., 138 (2008) 163.
14 D. G. Castner, K. Hinds and D. W. Grainger, Langmuir, 12 (1996) 5083.
15 M. M. Maye, J. Luo, Y. H. Lin, M. H. Engelhard, M. Hepel and C. J. Zhong, Langmuir, 19 (2003) 125.
16 M. C. Bourg, A. Badia and R. B. Lennox, J. Phys. Chem. B, 104 (2000) 6562.
17 M. J. Hostetler, J. E. Wingate, C. J. Zhong, J. E. Harris, R. W. Vachet, M. R. Clark, J. D. Londono, S. J. Green, J. J. Stokes, G. D. Wignall, G. L. Glish, M. D. Porter, N. D. Evans and R. W. Murray, Langmuir, 14 (1998) 17.
18 W. Jia, J. McLachlan, J. Xu, S. M. Tadayyon, P. R. Norton and S. H. Eichhorn, Can. J. Chem., 84 (2006) 998.
19 W. W. Weare, S. M. Reed, M. G. Warner and J. E. Hutchison, J. Am. Chem. Soc., 122 (2000) 12890.
20 C. Yee, M. Scotti, A. Ulman, H. White, M. Rafailovich and J. Sokolov, Langmuir, 15 (1999) 4314.
21 D. Li and J. Li, Colloids Surf., A, 257–258 (2005) 255.
22 L. Zhang, F. Huo, Z. Wang, L. Wu, X. Zhang, S. Hoeppener, L. Chi, H. Fuchs, J. Zhao, L. Niu and S. Dong, Langmuir, 16 (2000) 3813.
23 C. K. Yee, R. Jordan, A. Ulman, H. White, A. King, M. Rafailovich and J. Sokolov, Langmuir, 15 (1999) 3486.
24 F. P. Zamborini, S. M. Gross and R. W. Murray, Langmuir, 17 (2001) 481.
25 R. L. Whetten, J. T. Khoury, M. M. Alvarez, S. Murthy, I. Vezmar, Z. L. Wang, P. W. Stephens, C. L. Cleveland, W. D. Luedtke and U. Landman, Adv. Mater., 8 (1996) 428.H.
26 H. W. King and F. D. Manchester, J. Phys. F, 8 (1978) 15.
27 T. Teranishi and M. Miyake, Chem. Mater., 10 (1998) 594.
28 A. J. Kell, R. L. Donkers and M. S. Workentin, Langmuir, 21 (2005) 735.
29 P. D. Jadzinsky, G. Calero, C. J. Ackerson, D. A. Bushnell and R. D. Kornberg, Science, 318 (2007) 430.

DOI: 10.1007/s10973-008-9832-2